Application of GPR to Long Island Glacial Geology

Dan M. Davis
Department of Geosciences, State University of New York,
Stony Brook, NY 11794-2100

Introduction

Ground Penetrating Radar (GPR) is particularly well suited to use in dry, sandy, or cobble-poor sediments [e.g., McCann et al., 1988; Davis and Annan, 1989; Gawthorpe et al., 1993; Smith and Jol, 1995; Benson, 1995; Harari, 1996; Bristow et al., 1996; Daniels et al., 1998]. It has, however, been used in relatively few glaciogenic and aeolian dune or loess deposits [e.g., Schenk et al., 1993; Beres et al., 1995; Olsen and Andreasen, 1995; Sten et al., 1996]. I present here three examples of the application of GPR to Long Island glacial geology: a proglacial dune in the Grandifolia Sandhills of Baiting Hollow, a kettle hole with substantial loess deposits in Wildwood State Park, and areas of glaciotectonic thrusting at Hither Hills and on the USB campus (Figure 1). In each case, it is extremely useful to combine GPR surveys with other techniques and field observations. This is essential because, like seismic reflection and refraction data, GPR is much less effective at discriminating between different geologic media than it is at extrapolating their extent laterally away from where they have been characterized by other means. I therefore illustrate the use of GPR in conjunction with stratigraphic and grain-size analysis of hand-auger samples, mapping of exposed structures, and other techniques, such as multielectrode resistivity modeling.

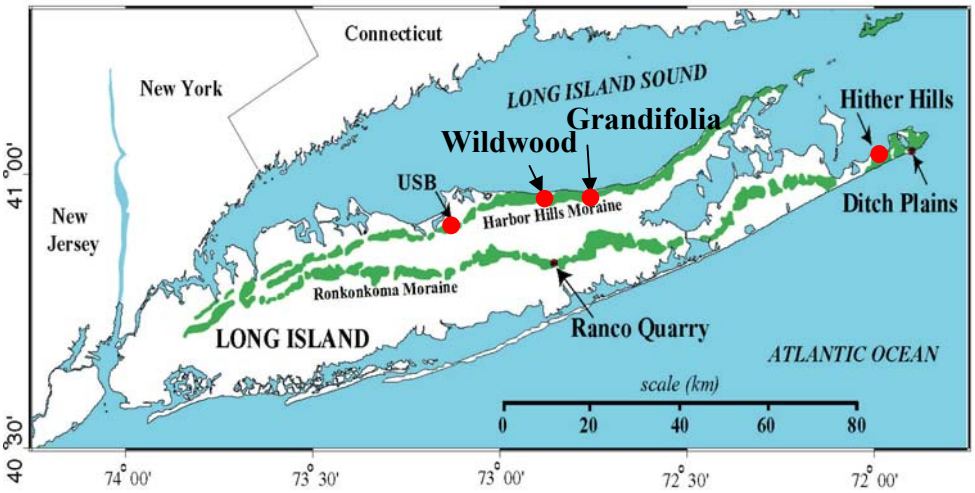

FIGURE 1: *Map of Long Island, showing the locations discussed in this abstract. GPR data from the Wildwood, Grandifolia, Hither Hills, and USB sites are shown in later figures.*

A GPR system operates using a matched pair of antennas. The transmitter antenna generates a radar signal and transmits it into the ground. After reflecting off objects in the subsurface, the signal is detected by the receiver antenna. Antenna sets are designated by their approximate peak signal frequency, measured in MHz (megahertz, or millions of cycles per second): ranging from tens of MHz, to about one GHz. Typical radar velocities in geological media range from around 15 cm/ns in dry sand to 8 cm/ns in glacial till and as low as 4 cm/ns in fully saturated sand [e.g., McCann et al., 1988; Gawthorpe et al., 1993].

In a raw radargram, stratigraphic layers appear as layers, but boulders or other point targets appear as hyperbolas. Radargrams replete with such hyperbolic reflectors are common in extremely poorly sorted sediments including cobbles and boulders, such as till. Hyperbolas are also found in radar lines that run across buried pipes or trees and their root systems. The shapes of these hyperbolas depend upon the radar velocity of the medium, making it possible to estimate that velocity. Radar velocity can also be estimated by semblance analysis and by the process of migration, which allows the conversion of a raw radargram (with travel time in the vertical axis) into a migrated radargram (with both axes representing distances in space). Better yet, direct measurement of the depth to an observed radar reflector with drilling of a hand auger can be used to convert observed 2-way signal travel times directly to velocities.

The spatial resolution it is possible to obtain with radar improves with increasing frequency. As a rule of thumb, resolution is about 1/4 the wavelength. The wavelength is simply the velocity divided by the frequency. For a typical velocity of 10 cm/ns, a 100 MHz antenna (0.1 cycles per nanosecond) therefore yields a 1-meter wavelength and a resolution of approximately 25 cm (10 inches). A low-frequency 25 MHz antenna will be unable to resolve objects of that size, having a resolution that is four times worse than for a 100 MHz antenna. Because attenuation (loss of signal energy) depends upon frequency, the signal from a 25 MHz antenna will penetrate farther into the earth than the signal from a higher-frequency antenna. Higher-frequency antennas have progressively worse depth of penetration, but better resolution. High frequency (400 to 800 MHz) antennas can resolve objects as small as 3-6 cm. Our 200 MHz antenna set provides the most useful combination of signal penetration and resolution for most initial surveys of near-surface features.

Pleistocene Dune

The Grandifolia Sandhills are located along the north shore of eastern Long Island in Baiting Hollow, New York (Figure 1). At their southern edge, the front of the hills display a lobate form, convex side to the south-southeast, with their steep 10-15 m relief stabilized by vegetation. Our survey site is on a ridge that is covered by a deciduous forest with a well-developed organic layer. Prominent among the trees is the species *Fagus grandifolia,* a type of dwarf beech tree for which the hills are named. Just to the south of the hills is diamict that we interpret as glacial till of the Harbor Hill moraine, or reworked material derived directly from the till without significant sorting. Where soil on the hills has been removed, the underlying sediment is well-sorted sand.

2a)

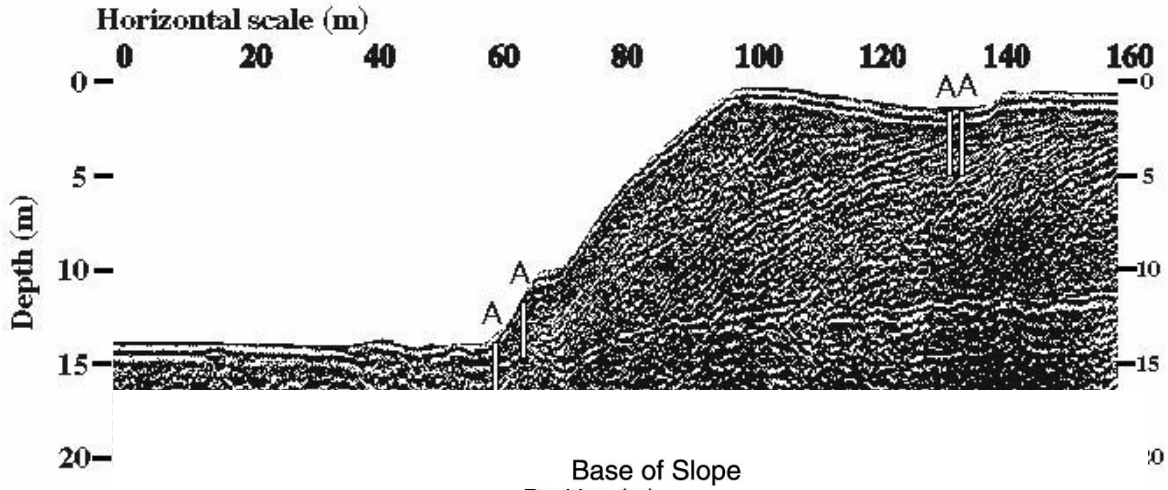

2b)

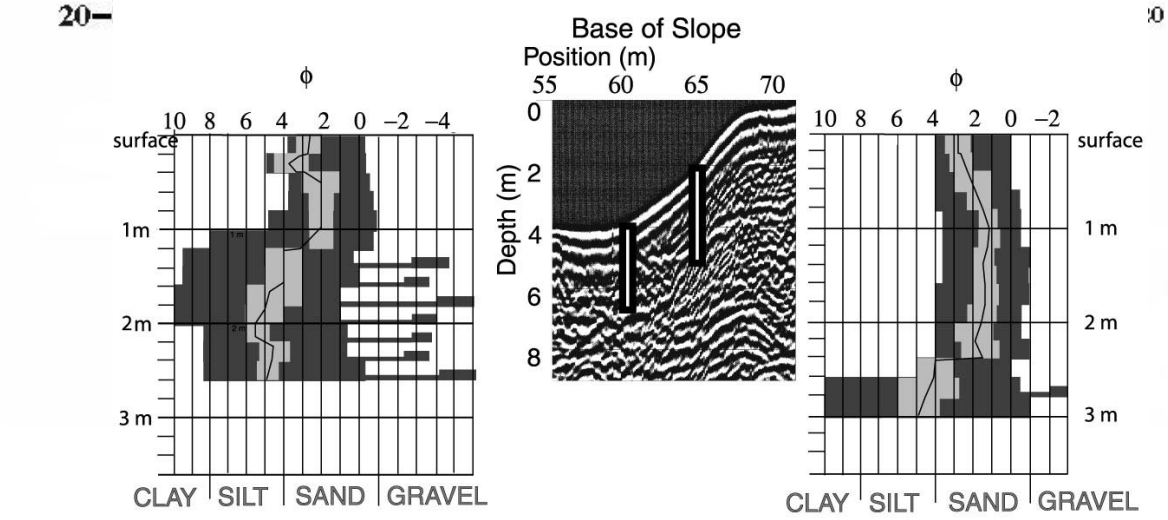

FIGURE 2: *Results of a combined GPR and sampling survey of a dune in the Grandifolia dune field, Baiting Hollow, Long Island.*

- ***2a)*** *Migrated radargram running roughly S-N across the frontal (southern) edge of a dune. I interpret the series of southward (leftward) diping layers within the dune to be slip surfaces associated with dune growth. Near the level of the plain to the south, a strong reflector continues beneath the entire dune. Auger analysis confirms this to be the contact with the till beneath the dune.*
- ***2b)*** *Results of Elliot Klein's sieve analysis of sediments from two auger holes near the base of the dune. Note the clear transition from well-sorted aeolian sands above to extremely poorly-sorted glacial till below the prominent reflector.*

Englebright et al. [2000] explain these lobate hills as parabolic dunes, which are commonly found in front of glaciers, convex side pointing downwind and away from the glacier [Collinson and Thompson, 1982; Lancaster, 1995; Benn and Evans, 1998]. Well-documented examples of such dunes are found in Alaska, Quebec, Colorado, Nebraska, Australia, eastern Europe, and The Netherlands, and their morphology has received considerable study [e.g., McKee, 1979; Collinson and Thompson, 1982; Thompson, 1983; Schenk, 1990; Fryberger, 1990, 1993; Muhs et al., 1996; Derbyshire and Owen, 1996; Zeeberg, 1998]. Parabolic dunes in the Hudson Valley, Eastern Great Lakes, and St Lawrence Valley [Filion, 1987; Dineen et al., 1988; Karrow and Occhietti, 1989; Thorson and Schile, 1995], have all been interpreted as the result of strong, dry northwesterly winds off the last of the retreating Pleistocene glaciers.

We have run a series of GPR profiles along the frontal (SE) portion of a lobate hill and onto the plain to the south. The main transect line is shown in Figure 2a. Raw radar images of the diamict in the plain have numerous overlapping hyperbolas due to a high density of cobbles. Migration of the radar data from there successfully 'collapses' the hyperbolas. The radar velocity is approximately 9 cm/ns, typical for till. The radar character of the top of the ridge is quite different. The lack of hyperbolic reflectors at depth indicates that below the surface of the ridge there are no sizeable buried objects (e.g., cobbles), consistent with our observation at the surface that this is well-sorted sand. We noted the location of each tree near the radar transect line and in each case observed the hyperbolic returns from the tree and its root system, finding a surficial velocity of about 15 cm/ns. The best velocity in the dipping sand layers is 14±1 cm/ns, typical of unsaturated sand. The sand and the till beneath it are separated by a very strong subhorizontal reflector that runs beneath the entire ridge at a radar depth of 160-190 ns (Figure 2a). Given the radar velocity of the sand, this means that the strong reflector separating the sand and the till is at a depth of close to 13m beneath the top of the ridge.

Short cross-lines and inflections in the main transect line yield a variety of apparent dips, allowing determination of the 3-D geometry of the dipping reflectors beneath the ridge. They appear, locally, to be nearly planar, with an ENE strike and a roughly southward dip of about 20°, typical for bounding surfaces in the nose of a parabolic dune [McKee and Bigarella, 1979]. Similar dipping layers, interpreted as bounding surfaces, have been observed in a dune GPR study in Colorado [Schenk et al., 1993]. Our observations of dune morphology and internal structure are therefore consistent with growth in the presence of strong winds from the NW or NNW, as well as with the shape and orientation of the hills [Reineck and Singh, 1975; Derbyshire and Owen, 1996; Lancaster, 1995; Benn and Evans, 1998].

Using a hand auger, we sampled to a depth of 3.6 m in two locations on the hill, penetrating about 1/3 of the way to the strong reflector (Fig. 2a), with nearly 100% sample recovery. The sediments consist entirely of moderately well to well sorted subrounded to rounded sand [Folk, 1968, Lewis, 1984], with subtle variations in mineralogy that apparently reflect variations in source. Grain size distributions are known to vary within individual dunes and, particularly, between dune fields [Lancaster, 1995]. The values we have measured are well within the range typical of such dunes [Ahlbrandt, 1979], although they have a relatively modest degree of sorting and are relatively coarse compared to some other aeolian dunes. This observation is consistent with a relatively proximal source, probably in glacially mobilized Cretaceous sandstone that was exposed to the north in what is now Long Island Sound (Fig. 1) during the Pleistocence.

Comparison with the radar data in Fig. 2a shows that these layers of known composition (pure sand) can be followed down-dip from the top of the ridge all of the way to the bright reflector. Similar radar layering is found throughout the rest of the ridge as well.

We placed an additional set of auger holes just above the base of the hill (Fig. 2b). Above the strong radar reflector, the sediments consist entirely of the same well-sorted sand as in the auger holes atop the hill. The layer responsible for the strong radar reflector was found to be ≈50 cm of very fine silt-to-clay matrix, with sand and interspersed cobbles. Analysis shows it to be very poorly sorted (a standard deviation of 2.45 around a mean ϕ of 3.58), with a marked fine-skewness of 0.25. The platykurtic kurtosis of 0.79 reflects its bimodal grain size distribution, with peaks in the $2 < \phi < 3$ (fine sand) and $7 < \phi < 9$ (very fine silt to clay) ranges. Sediment below this horizon was till, with a very poorly sorted (standard deviation of 2.13 around a mean ϕ of 1.71), symmetric (skewness of only 0.02) sediment size distribution. The very leptokurtic (2.46) kurtosis of this till is indicative of an abundance of fine sand, with silt and occasional cobbles. The largest of the recovered cobbles was close to the 5 cm maximum recoverable size. It was impossible to collect samples beyond a short distance into this thick lower till layer, apparently because the auger inevitably encountered cobbles that were too large to permit further penetration. Auger samples from the silt and clay layer and the sand directly above it were wet. Apparently the clay and silt-rich layer at the top of the till is a significant impediment to fluid drainage. The sharp contrast in sediment properties (from sand to till), combined with this perched water, explains the unusual prominence of the reflector (Fig. 2a) that we found at the sand/till interface beneath the entire imaged portion of the ridge.

Loess-filled Kettle

With a group of students led by Vesna Kundic, I have recently begun a coordinated GPR – resistivity – sedimentological survey of a glacial kettle hole in Wildwood State Park along the Harbor Hills Moraine in eastern Long Island (Figure 1). Loess deposits likely formed after the glacier retreated and proglacial lakes eventually drained to the sea. Substantial quantities of fine sediment would then have been available for aeolian transport, blowing and drifting across Long Island. Like dry blowing snow, it would likely accumulate in local topographic lows such as kettle holes. The ice that formed extremely large kettle holes may not have fully melted by the time of most intense availability of fine windblown sediment, and very small holes may not have provided significant shelter from the wind to allow significant loess accumulation. Graduate student Vesna Kundic and her advisor, Gil Hanson, settled on a medium-sized kettle hole in Wildwood State Park (Figures 1, 3a) as a likely site for her study of loess deposits.

Along with a group of students, we have carried out a series of GPR and multi-electrode resistivity surveys within this segmented kettle hole, which is elongate in shape (roughly 80 by 200 m) and about 12 m deep. Eight separate auger holes provide ground truth, verifying the presence of loess and establishing the depth to its base. Approximately 400 m of crossing radar lines allow us to extrapolate auger data laterally, mapping out the distribution of loess in 3 dimensions. We find that the loess is 2-3 meters deep in an area centered near the current bottom of the hole. Radar reflections are relatively weak (unlike our previous experience with loess at Caumsett State Park), but the contact between it and the till is easily traced (Figure 3b).

3a)

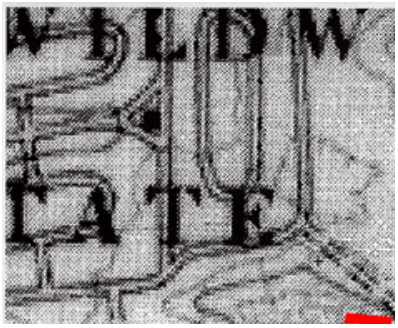

3b)

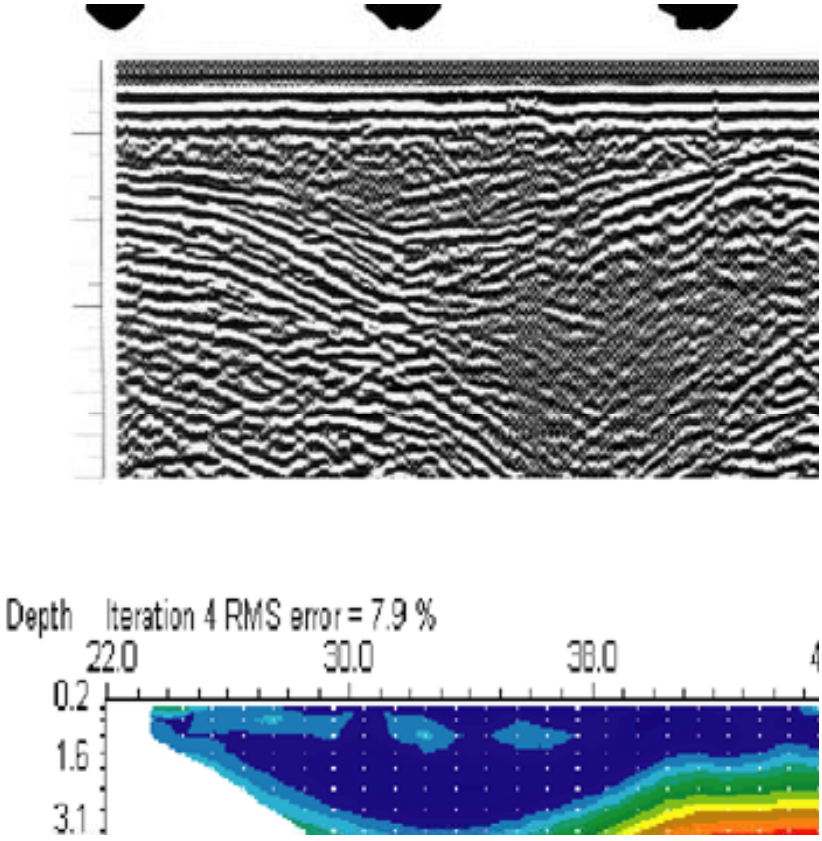

FIGURE 3: *Results of a survey using GPR, resistivity, and auger sampling in a kettle hole.*

3a) *Location of the kettle hole, near camping area 'E' in Wildwood State Park.*

3b) *Geophysical data from the kettle, and its interpretation:*

- *200 MHz GPR line, migrated but without topographic correction. Note the clear reflector along the top of the glacial material beneath the loess.*
- *2-D resistivity model at the same location as the GPR line in 3b. Note the strong contrast between the conductive loess and the resistive sediments beneath.*
- *Preliminary interpretation, based upon geophysical data and hand auger sampling.*

The top part of Figure 3b shows a 47 m segment near the eastern end of the 200 m main radar transect of the kettle hole system. Vertical exaggeration is approximately 2.5:1. The record has been migrated, but the topographic correction has not been applied. In reality, the surface slopes down to the right at an angle of roughly 5° to 7°. Note the boundary to radar-complex glacial material that is near 2 m depth across much of this part of the survey. That boundary approaches the surface near the left end of the area illustrated in Figure 3b,and also about 12 m from the left edge – a position 34 meters into the main E-W line. Variations that depth across the various radar lines have been verified using a hand auger. Sampling invariably encounters soil and tree roots very close to the surface, followed by uniform and extremely fine-grained sediment – loess. Auger sampling terminates where cobbles and boulders are encountered, rendering impossible any further progress with the auger.

The direct determination of depth to the top of the sediments beneath the loess using the auger makes it possible to estimate very accurately the radar velocity in the loess. The raw radargrams show many prominent hyperbolic reflections in that sediment, characteristic of boulders in till. The shape of those hyperbolas provide additional constraints on radar velocity, making it possible to migrate the raw data and produce radargrams in x-z (as opposed to x-time) space, such as the one in Figure 3b.

That segment of the 200 m transect line corresponds to one of our resistivity survey lines. Our resistivity system uses 48 electrodes, strung out along two cables. Electrode spacing can be as large as 5 m, but for this high-resolution shallow survey we used a 1-meter spacing, producing a 47 m total line length. The survey shown in Figure 3b is a dipole-dipole survey: Each of the 710 observations needed to produce this resistivity line consists of an electrode quadrupole: a current is run across one pair of electrodes and a voltage measured across another pair. Those data are then inverted using a finite element technique that allows the determination of a distribution of electrical resistivity at depth capable of best explaining the measured voltages.

The middle portion of Figure 3b is the result of a preliminary inversion of resistivity data along the same segment of the long radar line as depicted in the top segment of that figure. Note the close correspondence between the placement of the base of the loess using the two techniques. The loess is about an order of magnitude more conductive (less resistive) than the more porous and probably drier till beneath it. The bottom segment of Figure 3b is an interpretative sketch of that boundary and of the overall radar fabric of the deeper glacial material.

Glaciotectonic Thrusting

The moraines of Long Island, including the Harbor Hill Moraine on which the Stony Brook campus is built [Nieter et al., 1975; Fullerton et al., 1992], display a diverse range of push-moraine structures (e.g., Fig. 2). This deformation occurred on a scale intermediate between those of natural fold-and-thrust belts [Davis et al., 1983; Dahlen et al., 1984] and the laboratory models used by Davis and his students [Wang and Davis, 1996; Haq and Davis, 1997]. These push moraines provide an opportunity for more focused study of the conditions associated with

the glacial thrusting and folding that has so influenced the topography and hydrology of Long Island.

Several different styles of proglacial deformation have been reported in front of glaciers around the world [e.g., Boulton, 1986; Croot, 1988; Aber et al., 1989; Hart and Boulton, 1991], and in some cases this takes a form very similar to that of foreland fold-and-thrust belts. Composite push moraines can lead to the formation of multiple thrust-cored folds over a decollement [e.g., Croot, 1987; Lehmann, 1993]. Seasonal (or annual) push moraines have also been observed: they form as a glacier deposits new sediments each summer as it retreats and folds them during a partial readvance each winter [e.g., Boulton, 1986; Bennett and Glasser, 1996].

Hither Hills (Figure 1), which is part of the Ronkonkoma moraine, is on the South Fork of the island, 170 km east of New York City. It is a 5 km by 2 km area containing dozens of linear to slightly arcuate hills that display nearly uniform geometries within smaller areas or 'patches' of the study region. The heights and spacing of the hills vary somewhat from area to area, with hills typically about 10-15 meters above the troughs and approximately 80 to 200 meters between hill crests. Ridges can typically be traced along strike for distances of several hundred meters, and hill axes run mostly NE-SW. The bearings of each local 'patch' of hills are very consistent, and their topographic amplitudes and wavelengths are quite uniform.

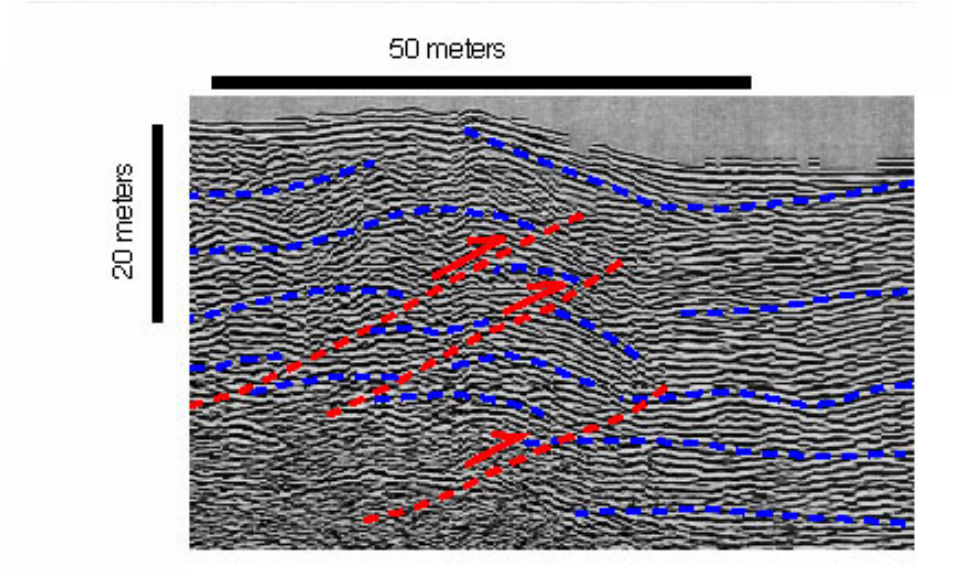

FIGURE 4: *Annotated radar line of thrust faulting at Hither Hills Park on the south fork of Long Island (Figure 1). Low-angle dashed lines indicate trends of reflector orientation. These reflectors fall into distinct dip domains: I interpret the boundaries between these domains to be thrust faults, dipping to the north (left). The distribution of these interpreted faults is consistent with the topographic relief of the E-W trending hills in that area. Similar structures have been observed beneath the hills in the Ashley Schiff Preserve (located on the USB campus just north of MSRC).*

The Hither Hills subparallel ridge and valley stream system is arcuate in plan and resembles a small composite-ridge system as described by Aber, although the ridge heights are smaller than the glaciotectonic landform they describe. Documented push-ridge systems commonly show an overall surface slope of a few degrees down toward the front [e.g., Croot, 1987; Lehmann, 1993; Hambrey, 1994], an overall geometry that has been attributed in the glacial literature [van der Wateren, 1995; Schlüchter et al., 1999] to 'critical wedge mechanics'. This mechanics [e.g., Davis et al., 1983; Dahlen et al., 1984, Byrne et al., 1993; Wang and Davis, 1996; Haq and Davis, 1997], allows us to draw inferences about the mechanical state of the material being deformed [e.g., Davis and von Huene, 1986].

The ridges in Hither Hills are larger than typical for terrestrial annual push-moraines documented by Boulton [1986], but the there resemble those described by Boulton as forming due to annual wintertime advance of a glacier during a time of overall retreat, a 'repeated push' (annual) model. In a preliminary survey, we have measured sections in an area where several ridges are transected by wave action along a beach [Klein et al., 1999]. We find considerable evidence for syntectonic deposition of sediments in miniature 'piggy-back' basins between the ridges. Strata in the cores of anticlines typically show greater fold amplitude than do shallower layers, which thicken away from the axes of the anticline-cored hills.

Conclusions

The ability of GPR to image the top few tens of meters below the surface in glacial sediments [Beres et al., 1995; Daniels et al., 1998] makes it an ideal complement to data obtained using resistivity and hand auger equipment on [Klein et al., 2000]. The geophysical techniques all for lateral extrapolation of localized and more traditional geological observations. The dry, porous nature of many Long Island sediments makes them ideal for study using GPR. More conductive, clay-rich sediments that restrict GPR are well suited to resistivity. A complete survey should use all available and appropriate methods.

References

Aber, J.S., D.G. Croot, and M.M. Fenton, Glaciotectonic Landforms and Structures, Kluwer Academic Publisher, 1989.

Ahlbrandt, T.S., 1979, Textural paramaters of eolian deposits, Chapter B, *in*, E.D. McKee (ed.), A Study of Global Sand Seas, p.21-51, U.S. Geological Survey Professional Paper 1052.

Benn, D.I., and D.J. A. Evans, Glaciers & Glaciation, 734 pp., Arnold Publishers, New York, 1998.

Bennett, M.S., and N.F. Glasser, Glacial Geology: ice sheets and landforms, John Wiley and Sons, New York, 1996.

Benson, A.K., Application of ground penetrating radar in assessing some geological hazards: examples of groundwater contamination, faults, cavities, *Journal of Applied Geophysics, 33*, 177-193, 1995

Beres, M., A. Green, P. Huggenberger, and H. Horstmeyer, Mapping the architecture of glaciofluvial sediments with three-dimensional georadar, *Geology, 23*, 1087-1090, 1995.

Bertran, P., B. Hétum J.-P. Texier, and H. van Steijn, Fabric characteristics of subaerial slope deposits, *Sedimentology, 44*, 1-16, 1997.

Boulton, G.S., Push-moraines and glacier-contact fans in marine and terrestrial environments, *Geomorphology, 33*, 677-698, 1986.

Bristow, C., J. Pugh, and T. Goodall, Internal structure of aeolian dunes in Abu Dhabi determined using ground-penetrating radar, *Sedimentology, 43*, 995-1003, 1996.
Byrne, D.E., Wang, W.-H., Davis, D.M., Mechanical Role Of Backstops in the Growth of Forearcs, *Tectonics, 12*, 123-144, 1993
Collinson, J.D., and D.B. Thompson, Sedimentary Structures, George Allen & Unwin, Ltd., London, 194 pp., 1982.
Croot, D.G., Glacio-tectonic structures: A mesoscale model of thin-skinned thrust sheets?, *J. Structural Geology, 9*, 797-808, 1987.
Croot, D.G., Glaciotectonics: Forms and processes, 212 p., A.A. Balkema, Rotterdam, 1988.
Dahlen, F. A., J. Suppe, and D. Davis, Mechanics of fold-and-thrust belts and accretionary wedges: Cohesive Coulomb theory, *J. Geophys. Res., 89*, 10087-10101, 1984.
Daniels, J.J., J. Brower, and F. Baumgartner, High-resolution GPR at Brookhaven National Laboratory to delineate complex subsurface targets, *J. Environmental & Engineering Geophysics, 3*, 1, 1-6, 1998.
Davis, J.L., and A.P. Annan, Ground-penetrating radar for high resolution mapping of soil and rock stratigraphy, *Geophysical Prospecting, 37*, 531-551, 1989.
Davis, D., Suppe, J., and Dahlen, F.A., Mechanics of fold-and-thrust belts and accretionary wedges, *J. Geophys. Res., 88*, 1153-1172, 1983.
Davis, D.M. and R. von Huene, Inferences on sediment strength and fault friction from structures at the Aleutian Trench, *Geology, 15*, 517-522, 1987.
Derbyshire, E., and L.A. Owen, Glacioaeolian processes, sediments and landforms, Chapter 6 (p. 213-237), *in, Past Glacial Environments: Sediments, Forms and Techniques, Glacial Environments: Volume 2*, edited by J. Menzies , Butterworth-Heinemann Ltd., Oxford, 1996.
Dineen, R.J., D.J. DeSimone, and E.L. Hanson, Glacial Lake Albany and its successors in the Hudson Lowlands, in Amer. Quaternary Assoc. Meeting Field Trip Guidebook, 1988, Amherst, MA, Amer. Quaternary Assoc., p. 15-16, 1988
Engelbright, S.C., G.N. Hanson, T. Rasbury, and E.E. Lamont, On the origin of parabolic dunes near Friar's Head, Long Island, New York, *Long Island Botanical Society: The Quarterly Newsletter, vol. 10*, no. 1, Jan.-Mar., 2000, LI Botanical Society, E. Norwich, NY, 2000.
Filion. L., Holocene development of parabolic dunes in the central St. Lawrence lowland, Québec, *Quaternary Research, 28*, 196-209, 1987.
Fullerton, D.S. and 9 others, Quaternary Map of the Hudson River 4° x 6° Quadrangle, United States and Canada, Map I-1420, U.S. Department of the interior, U.S.G.S., 1992
Fryberger, S.G., Eolian Stratification, *in* S.G. Fryberger, L.F. Krystinik, an C.J. Schenk (eds.), *Modern and Ancient Eolian Deposits*: Petroleum Exploration and Production, Rocky Mtn, Section, Society of Economic Paleontoogists and Mineralogists, Chapter 4, 12pp, 1990.
Gawthorpe, R.L., R.E. Ll Collier, J. Alexander, J.S. Bridges, and M.R. Leeder, Ground penetrating radar: application to sandbody geometry and heterogeneity studies, *in*, C.P. North and D.J. Prosser (eds.), *Characterization of Fluvial and Aeloian Reservoirs*, Geological Society Special Publication No. 73, The Geological Society, London, pp. 421-432, 1993.
Harari, Z., Ground-penetrating radar (GPR) for imaging strtigraphic features and groundwater in sand dunes, *J. Applied Geophysics, 36*, 43-52, 1996.
Hambrey, M., Glacial Environments, University of British Columbia Press, Vancouver, 1994
Haq, S.S.B. and D.M. Davis, Oblique convergence and the lobate mountain ranges of western Pakistan, *Geology, 25,* 23-26, 1997.
Hart, J.K., and G.S. Boulton, The interrelation of glaciotectonic and glaciodepositional processes within the glacial environment, *Quaternary Science Reviews, 10*, 335-350, 1991.
Karrow, P.F. and S. Occhietti, Quaternary geology of the St. Lawrence lowlands of Canada, *in*, R.J. Fulton (ed.), Quaternary Geology of Canada and Greenland, GSA Geology of North Aerica series v. K-1, 321-389, 1989.
Klein, E.C., and D.M. Davis, Glaciotectonic Processes and Glacigenic Sediments on Eastern Long Island, Conference on the Geology of Long Island and Metropolitan New York, Stony Brook, NY, April 24, 1999.
Klein, E,C., F.A. Winslow III, D.M. Davis, and W.E. Holt, First Steps at the Ground Penetrating Radar Mapping of the Shallow Subsurface Geology, Hither Hills, Eastern Long Island, Conference on The Geology of Long Island and Metropolitan New York, Stony Brook, NY, April 15, 2000.
Lancaster, N., *Geomorphology of Desert Dunes*, 290 pp., Routledge, New York, 1995.
Lehmann, R., The significance of permafrost in the formation and appearance of push moraines, Cheng Guodong (chairperson), Permafrost; sixth international conference proceedings, International Conference on Permafrost, Proceedings, 6, Vol. 1, p. 374-379, 1993., Beijing, China, July 5-9, 1993.
McCann, D.M., Jackson, P.D., and Fenning, P.J., Comparison of the seismic and ground probing radar methods in geological surveying, *IEE Proc*. 135, 380-390, 1988.

McKee, E.D., Introduction to a study of global sand seas, in McKee, E.D., (ed.), A Study of Global Sand Seas, 3-19, United States Geological Survey, Professional Paper 1052, 1979.

McKee, E.D. and J. J. Bigarella, Sedimentary structures in dunes, With sections on The Lagoa dune field, Brazil, Chapter E, , *in*, E.D. McKee (ed.), A Study of Global Sand Seas, p.83-139, U.S. Geological Survey Professional Paper 1052, 1979.

Meyers, W.J., Boguslavsky, S., Dunne, S., Keller, J., Lewitt, D., Lani, M., McVicker, A., and Cascione, Matituck Cliffs and Ranco Quarry: Models for Origin of Roanoke Point and Ronkonkoma Moraines?, *Conf. On Geology of Long Island and Metropolitan NY*, 83-90, April 1998.

Muhs, D.R., T.W. Stafford, S.D. Cowherd, S.A. Mahan, R. Kihl, P.B. Mat, C.A. Bush, J. Nehring,Origin of the late Quaternary dune fields of northeastern Colorado, *Geomorphology, 17*, 129-149, 1996.

Nieter, W., B. Nemickas, E.J. Koszalka, and W.S. Newman, The Late Quaternary Geology of the Montauk Peninsula, Montauk Point to Southampton, Long Island, New York, p. 129-1553, in New York State Geological Association Guidebook, 47th Annual Meeting, 1975.

Olsen, H., and F. Andreasen, Sedimentology and ground-penetratiing radar characteristics of a Pleistocene sandur deposit, *Sedimentary Geology, 99*, 1-15, 1995.

Reineck, H.-E., and I.B. Singh, Depositional Sedimentary Environments, Springer-Verlag, New York. 439 pp., 1975.

Schenk, C.J., Eolian dune morphology and wind regime, *in* S.G. Fryberger, L.F. Krystinik, an C.J. Schenk (eds.), *Modern and Ancient Eolian Deposits*: Petroleum Exploration and Production, Rocky Mtn, Section, Society of Economic Paleontoogists and Mineralogists, Chapter 3, 8pp, 1990.

Schenk, C.J., Gautier, D.L., Olhoeft, G.R., and Lucius, J.E., Internal structure of an aeolian dune using ground-penetrating radar, *in, Aeolian Sediments: Ancient and Modern*, edited by Pye, K., and Lancaster, N., Special Publication Number 16 of the International Association of Sedimentologists, Blackwell Scientific Publications, Oxford, p. 61-69, 1993.

Schlüchter, C., Gander, P., Lowell, T.V., and Denton, G.H., Glacially Folded Outwash Near Lago Llanquihue, Southern Lake District, Chile, Geografiska Annaler, 81A, 347-358, 1999

Smith, D.G., and H.M. Jol, Ground penetrating radar: antenna frequencies and maximum probable depths of penetration in Quaternary sediments, *J. Applied Geophysics, 33*, 93-100, 1995.

Sten, E,, H. Thybo, and N. Noe-Nygaard, Resistivity and georadar mapping of lacustrine and glaciofluvial sediments in the late-glacial to postglacial Store Åmose basin, Denmark, *Bulletin of the Geological Society of Denmark, 43,* 87-98, 1996.

Thompson, C.H., Development and weathering of large parabolic dune systems aloong the subtropical coast of eastern Australia, *Z. Geomorph. N.F., 45*, 205-225, 1983.

Thorson, R.M., Schile C.A., Deglacial eolian regimes in New England, *Geological Society of American Bulletin, 107*, 751-761, 1995.

van der Wateren, D.F.M., Processes of glaciotectonism, in: J. Menzies (ed.) Modern Glacial Environments: Processes, Dynamics, and Sediments, Glacial Environments: Vol. 1, Butterworth Heinemann, Oxford, 1995.

Wang, W.-H. and Davis, D.M., Sandbox model simulation of forearc evolution and noncritical wedges *J. Geophys. Res*., 101, 11329-11339, 1996.

Zeeberg, J., The European sand belt in eastern Europe – and comparison of Late Glacial dune orientation with GCM simulation results, *Boreas, 27*, 127-139, 1998.